ISSN 0023-1584, Kinetics and Catalysis, 2009, Vol. 50, No. 2, pp. 220–227. © Pleiades Publishing, Ltd., 2009.
Original Russian Text © N.N. Tomina, P.A. Nikul'shin, V.S. Tsvetkov, A.A. Pimerzin, 2009, published in Kinetika i Kataliz, 2009, Vol. 50, No. 2, pp. 233–241.

Thiophene Hydrodesulfurization and Diesel Fuel Hydrorefining Activities of XMo$_6$(S)/γ-Al$_2$O$_3$ and Ni-XMo$_6$(S)/γ-Al$_2$O$_3$ (X = Al, Ga, In, Fe, Co, and Ni) Catalysts

N. N. Tomina, P. A. Nikul'shin, V. S. Tsvetkov, and A. A. Pimerzin

Samara State Technical University, Molodogvardeiskaya ul. 224, Samara, 443100 Russia
e-mail: pavel_nikulshin@mail.ru

Received July 25, 2007

Abstract—XMo$_6$(S)/γ-Al$_2$O$_3$ and Ni-XMo$_6$(S)/γ-Al$_2$O$_3$ catalysts based on Anderson heteropoly compounds (HPCs), where X = Al, Ga, In, Fe, Co, and Ni, were synthesized. The nature of the precursor HPC determines the activity of the catalysts in thiophene hydrogenolysis and diesel fuel hydrorefining in a flow-through setup. The activity of Ni-XMo$_6$(S)/γ-Al$_2$O$_3$ with X = Al, Ga, and In in diesel fuel dehydrosulfurization increases in the order Al < Ga < In. For catalysts in which the heteroatom is an element of the iron triad, the order of the increasing activities is Fe < Co < Ni. The highest activity in both reactions was observed for catalysts based on InMo$_6$-HPC and NiMo$_6$-HPC: the residual sulfur in the hydrogenizates obtained over them at 320°C was 2.5 times lower than over a conventional ammonium paramolybdate–based catalyst, whereas the degree of hydrogenation of polycyclic aromatic hydrocarbons (PAH) was 15–16 rel. % higher.

DOI: 10.1134/S0023158409020116

Heteropoly compounds (HPCs) in catalysis are a fruitful and interesting field for new synthetic possibilities in the design of catalysts. Heteropoly compounds provided considerable progress in understanding the catalytic effect of HPCs on the molecular level and in creation of a number of new full-scale processes [1]. Heteropoly compounds have unique physicochemical properties. Catalysts on their basis have a definite and well-known structure, efficiently enhance both acid and oxidative reactions, and frequently exceed state-of-the-art analogues in activity and/or selectivity.

It is promising to use HPCs as active phases (or precursors of active phases) for catalysts in hydrocatalytic processes. Various researchers studied HPCs as applied to synthesis or hydrogenation [2–5] and hydrorefining [6–23] catalysts.

12-Heteropolyacids with Keggin anions are used worldwide. Molybdenum and tungsten heteropolyacids (HPAs) with central atoms such as phosphorus and silicon are encountered most frequently. Most documentation concerns their properties. The results of their use in the synthesis of hydrorefining catalysts are found in [6–15].

Unsaturated 6-HPAs (Anderson structures) are not so widely used in catalytic hydrorefining reactions [16–23]. Pioneering works concerning the physicochemical and catalytic properties of these compounds appeared only at the beginning of the 21st century [17–20]. Our interest in these compounds is due to the variety of elements of the Periodic Table, including 3*d* metals that can serve as heteroatoms. Therefore, it was of interest to ascertain the activity of hydrorefining catalysts with various heteroatoms.

HPCs used in previous research were either $(NH_4)_3[Co(OH)_6W_6O_{18}] \cdot 7H_2O$ (CoW$_6$-HPC) and $(NH_4)_4[Ni(OH)_6W_6O_{18}] \cdot 5H_2O$ (NiW$_6$-HPC) [16] or $(NH_4)_3[Co(OH)_6Mo_6O_{18}] \cdot 7H_2O$ (CoMo$_6$-HPC) [17–19]. Many HPCs with various heteroatoms have not received attention.

However, many promising results have been obtained in this field [16–20]. Maitra et al. [16], for example, a discovered high hydrodesulfurization activity (for thiophene) in catalysts prepared on the basis of CoW$_6$-HPC and NiW$_6$-HPCs, but a low (compared to full-scale catalysts) hydrodenitrogenation activity (for quinoline) and, in some cases, hydrogenation activity (for phenanthrene). Noteworthy, Maitra et al. [16] compared catalysts containing the same MoO_3 proportion but different promoter proportions; that is, Maitra et al. knowingly used nonoptimal atom ratios between active components.

CoMo$_6$-HPCs were studied in [17–20]. Cabello et al. [17] studied the influence of the CoMo$_6$-HPC and 6-molydotellurate (TeMo$_6$-HPC) on the catalytic activity. Cabello et al. [17] studied HPC adsorption isotherms from aqueous solutions and inferred the Langmuir adsorption type and a possible planar location of the HPCs on the support surface. Varying the CoMo$_6$-HPC/TeMo$_6$-HPC weight ratio in the synthesis of catalysts and cancelling out the tellurium influence, Cabello et al. arrived at the conclusion that the increasing Co/Mo atom ratio enhances both hydrodesulfurization

(for thiophene) and hydrogenation (for cyclohexane) activities. This effect can be interpreted as resulting from the optimized atom ratio between active components.

The higher activity of HPC-based catalysts can be explained by an enhanced dispersion of the oxomolybdenum phase after calcination and direct molecular interactions between active components (Mo and Co(Ni)), which inhibit the migration of promoter atoms into the support [23] and depend on the type and electronic state of the heteroatom in the HPC [20].

In this work, we used HPCs containing iron triad elements (Fe, Co, or Ni) and boron-family elements (Al, In, or Ga) to prepare supported hydrorefining catalysts. We synthesized both unprotomoted $X\text{Mo}_6(\text{S})/\gamma\text{-Al}_2\text{O}_3$ samples and nickel-promoted $\text{Ni-}X\text{Mo}_6(\text{S})/\gamma\text{-Al}_2\text{O}_3$ catalysts. In this way, we ascertained the influence of the promoter and heteroatom on the catalytic activity and prepared systems with an optimal atom ratio between active components.

EXPERIMENTAL

The support used was $\gamma\text{-Al}_2\text{O}_3$ prepared from commercially available aluminum hydroxide (prepared by continuous precipitation from sulfate solutions) using extraction molding, drying, and calcining [21]. The texture characteristics of the thus-prepared alumina sample were determined by nitrogen adsorption at 77 K on a Micromeritics ASAP 2020 adsorption porosimeter. The specific surface area of this sample was 315 m^2/g; the effective pore size was 110 Å. Catalysts were manufactured by impregnating the 0.25–0.50 mm $\gamma\text{-Al}_2\text{O}_3$ fraction with active component solutions to the ultimate water capacity.

The impregnators used were ammonium paramolybdate $(NH_4)_6Mo_7O_{24} \cdot 4H_2O$ (APM), ammonium 6-molybdonickelate(II) $(NH_4)_4[Ni(OH)_6Mo_6O_{18}] \cdot nH_2O$ ($NiMo_6$-HPC), ammonium 6-molybdoferrate(III) $(NH_4)_3[Fe(OH)_6Mo_6O_{18}] \cdot nH_2O$ ($FeMo_6$-HPC), ammonium 6-molybdocobaltate(II) $(NH_4)_4[Co(OH)_6Mo_6O_{18}] \cdot nH_2O$ ($CoMo_6$-HPC), ammonium 6-molybdoaluminate(III) $(NH_4)_3[Al(OH)_6Mo_6O_{18}] \cdot nH_2O$ ($AlMo_6$-HPC), ammonium 6-molybdogallate(III) $(NH_4)_3[Ga(OH)_6Mo_6O_{18}] \cdot nH_2O$ ($GaMo_6$-HPC), and ammonium 6-molybdoindate(III) $(NH_4)_3[In(OH)_6Mo_6O_{18}] \cdot nH_2O$ ($InMo_6$-HPC). The HPCs were prepared by original or modified procedures as described in [24, 25]. IR spectra were recorded for crystalline HPC samples dried at 110°C and pelletized with KBr on an Avatar-360 FTIR spectrometer. These IR spectra are displayed in Fig. 1. The phase compositions of the precursor HPCs and catalysts were determined on a DRON-2 X-ray diffractometer ($\text{Cu}K_\alpha$ radiation).

Unpromoted catalysts of set I ($X\text{Mo}_6(\text{S})/\gamma\text{-Al}_2\text{O}_3$) were prepared using aqueous acid solutions of the corresponding HPCs (samples I-2 to I-7). An APM-based catalyst (sample I-1) was used as the reference for this set.

Promoted catalysts of set II ($\text{Ni-}X\text{Mo}_6(\text{S})/\gamma\text{-Al}_2\text{O}_3$) were prepared using joint aqueous solutions of the same HPCs and analytical grade $Ni(NO_3)_2 \cdot 6H_2O$ (samples II-9 to II-14). Here, the reference sample was the catalyst prepared by coimpregnation with APM and $Ni(NO_3)_2 \cdot 6H_2O$ (sample II-8).

The catalysts were dried at 80, 100, and 120°C for 2 h at each temperature and then calcined at 400°C for 2 h. Then, the catalysts in the oxide form were sulfidized as follows. Catalyst samples (0.25–0.5 mm fraction) were impregnated with di-*tert*-butyl polysulfide (54 wt % S), transferred to a separate glass reactor, and sulfidized for 2 h at atmospheric hydrogen pressure and 350°C. The optimal sulfidization parameters were determined earlier [26]. Table 1 lists the active component and sulfide sulfur percentages in catalysts before and after they were tested in a flow reactor.

All catalysts were tested for thiophene hydrogenolysis activity on a pulsed microcatalytic setup within 300–400°C in 20-K steps. The catalyst sample size was 25 mg; the thiophene volume was 0.2 μl. Reaction products were analyzed by gas-liquid chromatography (quartz capillary column with the OV-101 immobilized phase). Chromatograms were recorded and processed on a PC using UniChrom-97 v.4.3 software. The chromatograph was interfaced with the PC via an Lnet analog/digital converter, which measured the current signal directly on the flame-ionization detector.

Set II catalysts were also tested in a laboratory flow reactor under hydrogen pressure. The temperature in the reactor was adjusted with an accuracy of ±2 K, pressure with an accuracy of ±0.05 MPa, feed flow rate with an accuracy of ±0.2 ml/h, and hydrogen flow rate with an accuracy of ±0.2 l/h. The feed used in hydrorefining was 50 vol % directly distilled diesel fuel + 5 vol % light gasoil (catalytic cracking). The test parameters were as follows: temperature, 320, 340, 360, and 380°C; pressure, 4.0 MPa; feed flow rate, 2.0 h^{-1}; hydrogen : reagent ratio, 600 nl/l; and catalyst volume, 10 cm^3. Table 2 displays the characteristics of the feed and hydrogenizates. Total sulfur in the batch and hydrogenizates was determined by the lamp technique. Polycyclic aromatic hydrocarbons (PAH) were determined on a Shimadzu UV-1700 spectrophotometer according to [27].

The catalytic activity was ascertained as the degree of desulfurizing (hydrodesulfurization activity; HDSA) and the degree of PAH hydrogenation (hydrogenation activity; HA). The coke percentage in spent catalysts was determined by quantitative oxidation to CO_2, which was subsequently determined by gas chromatography. Sulfide sulfur in spent catalysts was determined as in [28]. The sulfur and coke percentages are listed in Table 1.

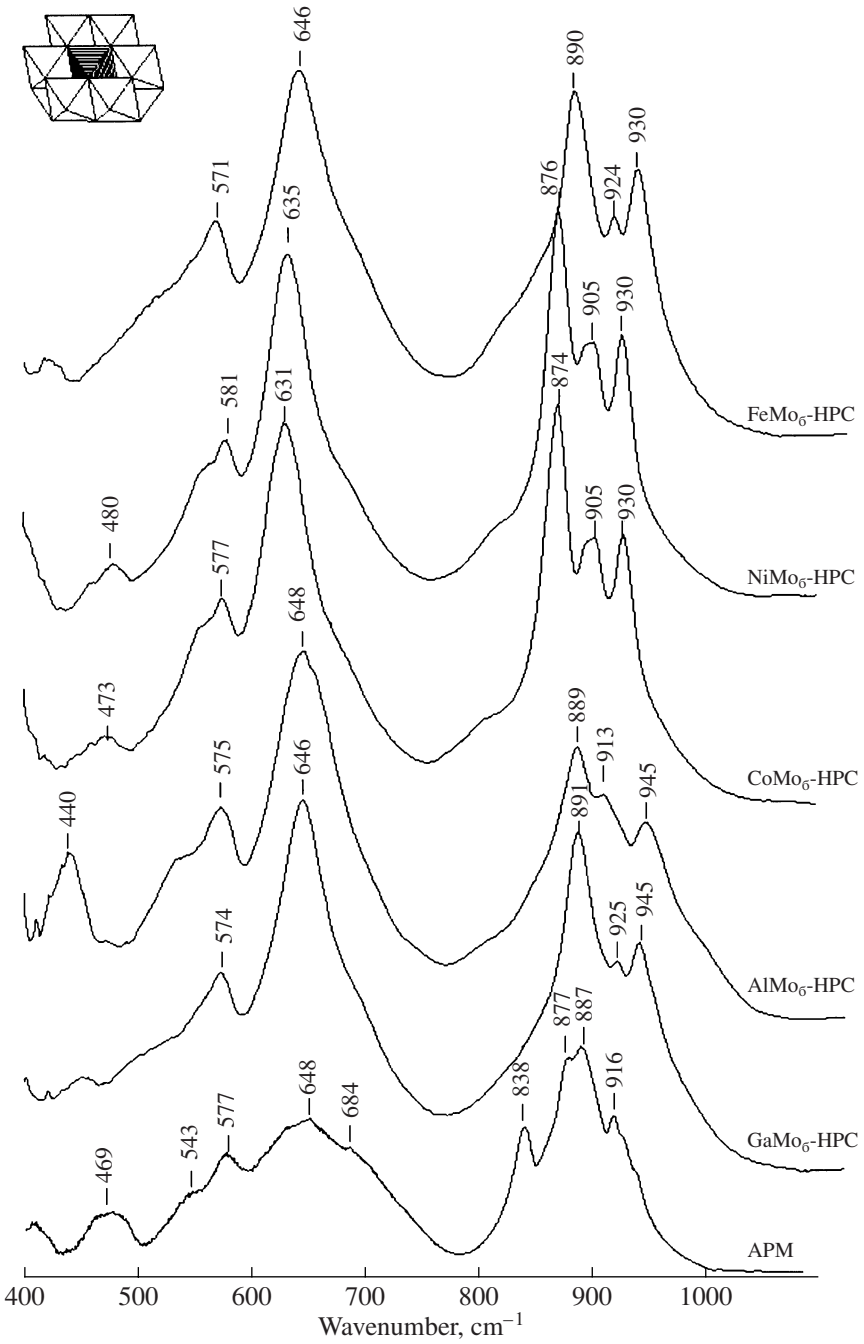

Fig. 1. IR spectra of Anderson HPCs dried at 110°C.

RESULTS AND DISCUSSION

The atom ratio Mo : *X* in our synthesized catalyst samples was about six as determined by quantitative analysis. Figure 1 displays IR spectra for HPCs. The characteristic bands for 6-HPCs coincide with previous descriptions [29–31]. Strong absorption bands within 950–880 cm^{-1} are associated with *cis*-MoO_2 bonds; those within 650–450 cm^{-1}, with Mo–O–Mo bonds.

X-ray powder diffraction showed that the HPCs have a complex crystal structure and are isomorphic. Their interplanar spacings coincide with the published values [32, 33].

Unpromoted $XMo_6(S)/\gamma\text{-}Al_2O_3$ catalysts differ from one another only in heteroatom *X*. The influence of the heteroatom on the catalytic activity was evaluated as the degree of thiophene conversion under identical hydrogenolysis conditions.

The $XMo_6(S)/\gamma\text{-}Al_2O_3$ catalysts with *X* = Al, Ga, or In had almost identical thiophene hydrogenolysis activities; samples I-3 and I-1 were noticeably more active

Table 1. Compositions of $X\mathrm{Mo_6(S)/\gamma\text{-}Al_2O_3}$ and Ni-$X\mathrm{Mo_6(S)/\gamma\text{-}Al_2O_3}$ catalysts before and after tests

Set	Molybdenum compound used in catalyst synthesis	Percentage in the catalyst, wt %					Percentage sulfiding of MoO_3 and metal oxide, rel. %
		MoO_3	NiO	sulfur		coke after test*	
				after sulfiding	after test*		
Catalysts $X\mathrm{Mo_6(S)/\gamma\text{-}Al_2O_3}$							
I-1**	APM	15.9	–	5.2	–	–	73.6
I-2	$\mathrm{AlMo_6}$-HPC	14.8	–	3.9	–	–	59.3
I-3	$\mathrm{GaMo_6}$-HPC	15.9	–	3.3	–	–	48.1
I-4	$\mathrm{InMo_6}$-HPC	14.8	–	3.4	–	–	50.2
I-5	$\mathrm{FeMo_6}$-HPC	14.4	–	3.5	–	–	54.7
I-6	$\mathrm{CoMo_6}$-HPC	15.3	–	4.9	–	–	72.1
I-7	$\mathrm{NiMo_6}$-HPC	15.2	1.3	3.3	–	–	48.8
Catalysts Ni-$X\mathrm{Mo_6(S)/\gamma\text{-}Al_2O_3}$							
II-8***	APM + Ni	15.2	3.2	3.7	4.8	2.1	46.0
II-9	$\mathrm{AlMo_6}$-HPC + Ni	14.6	3.6	3.6	5.8	2.5	51.1
II-10	$\mathrm{GaMo_6}$-HPC + Ni	15.8	3.8	3.2	5.9	6.8	55.5
II-11	$\mathrm{InMo_6}$-HPC + Ni	15.9	3.2	3.8	4.9	6.4	58.1
II-12	$\mathrm{FeMo_6}$-HPC + Ni	14.1	3.6	3.6	5.0	11.4	64.1
II-13	$\mathrm{CoMo_6}$-HPC + Ni	14.9	3.5	3.5	4.4	2.6	49.3
II-14	$\mathrm{NiMo_6}$-HPC + Ni	14.9	4.0	4.5	6.6	1.5	54.0

*Tests in a flow reactor for 12 h.
**$\mathrm{Mo_7(S)/\gamma\text{-}Al_2O_3}$ catalysts.
***Ni-$\mathrm{Mo_7(S)/\gamma\text{-}Al_2O_3}$ catalysts.

only at high temperatures (Fig. 2a). Apparently, chemical reactions between molybdenum compounds and alumina in the course of drying, calcining, and sulfidizing produced immobilized sulfide phases with similar activities.

Figure 2b plots thiophene conversion versus reaction temperature over set I catalysts with X = Fe, Co, and Ni and over the reference. The thiophene conversion over the $\mathrm{FeMo_6}$-HPC catalyst (sample I-5) was lower than over the $\mathrm{Mo_7(S)/\gamma\text{-}Al_2O_3}$ conventional reference (sample I-1). A higher activity was observed for sample I-6; sample I-7, which was synthesized using $\mathrm{NiMo_6}$-HPC, was the most active catalyst. Noteworthy, our data on thiophene hydrogenolysis over $\mathrm{NiMo_6}$-HPC

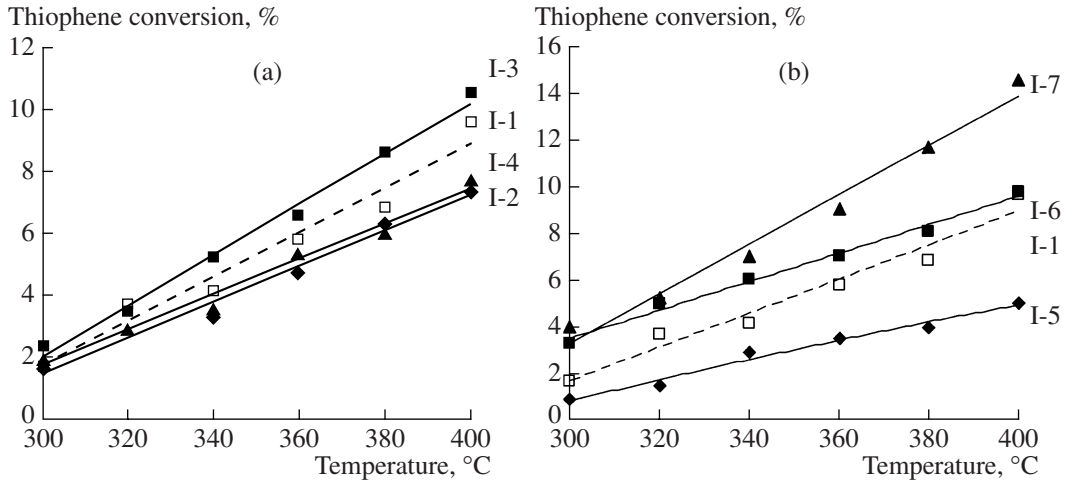

Fig. 2. Thiophene conversion versus temperature for Anderson HPC–based $X\mathrm{Mo_6(S)/\gamma\text{-}Al_2O_3}$ catalyst samples (a) I-2 to I-4 and (b) I-5 to I-7 and over an APM-based $\mathrm{Mo_7(S)/\gamma\text{-}Al_2O_3}$ catalyst (I-1).

Table 2. Physicochemical properties of hydrogenizates

Set and catalyst no.	T, °C	ρ_4^{20}, g/cm^3	n_D^{20}	Residual weight percentage, wt %		
				sulfur	BAH*	TAH**
Precursor		0.8779	1.4915	1.090	9.64	4.37
II-8	320	0.7961	1.4890	0.295	5.05	2.40
	340	0.8699	1.4880	0.250	4.76	2.49
	360	0.8579	1.4860	0.125	5.09	2.52
	380	0.8553	1.4850	0.080	6.33	2.56
II-9	320	0.8621	1.4820	0.260	6.01	1.99
	340	0.8638	1.4830	0.190	5.62	2.13
	360	0.8647	1.4825	0.100	5.59	2.16
	380	0.8599	1.4815	0.060	6.11	2.26
II-10	320	0.8631	1.4795	0.229	4.80	1.85
	340	0.8585	1.4791	0.111	5.08	2.26
	360	0.8574	1.4795	0.065	6.09	2.09
	380	0.8601	1.4795	0.035	6.46	2.57
II-11	320	0.8565	1.4765	0.116	5.76	1.02
	340	0.8585	1.4790	0.070	4.55	1.24
	360	0.8541	1.4795	0.043	3.49	1.67
	380	0.8622	1.4805	0.022	4.68	1.83
II-12	320	0.8601	1.482	0.211	5.79	2.27
	340	0.8609	1.4825	0.158	5.88	2.19
	360	0.8696	1.4819	0.118	5.45	2.21
	380	0.8565	1.4826	0.075	6.21	2.77
II-13	320	0.8633	1.4825	0.196	7.27	2.31
	340	0.8656	1.4830	0.150	6.51	2.60
	360	0.8623	1.4836	0.080	5.41	2.62
	380	0.8641	1.4845	0.069	7.28	2.88
II-14	320	0.8636	1.4835	0.120	4.13	1.50
	340	0.8615	1.4825	0.059	3.89	1.59
	360	0.8608	1.4810	0.032	4.98	2.18
	380	0.8603	1.4810	0.020	6.13	2.34

*Bicyclic aromatic hydrocarbons.

**Tricyclic aromatic hydrocarbons.

and $CoMo_6$-HPC completely agree with those of Pettiti et al. [20].

The composition of promoted Ni-XMo$_6$(S)/γ-Al_2O_3 catalysts also differed from one another only in heteroatom X. Therefore, in ascertaining the differences between the properties of these catalysts, we in fact determined how the HPC, more exactly, the heteroelement, influences the properties of the catalysts.

Thiophene conversion over set II catalysts with X = Al, Ga, or In was roughly the same as on XMo$_6$(S)/γ-Al_2O_3 (Fig. 3a). Over Ni-XMo$_6$(S)/γ-Al_2O_3 catalysts with X = Fe, Co, or Ni, different dependences were obtained (Fig. 3b). At high temperatures, catalyst II-14 was more active than the others. Sample II-13 had the highest activity at low and moderate test temperatures; the catalysts synthesized from $FeMo_6$-HPC were again less active.

Diesel fuel hydrorefining over set II catalysts gave the following results. Sample II-11, prepared with the use of $InMo_6$-HPC, was the most active catalyst of the Ni-XMo$_6$(S)/γ-Al_2O_3 set with X = Al, Ga, and In (Fig. 4a). The reference (sample II-8) had a lower activity than all test catalysts: its HDSA was 89.6 rel. % at 320°C and 98.0 rel. % at 380°C.

Comparing the hydrogenation activities of set II catalysts with X = Al, Ga, and In (Fig. 4b), we found the

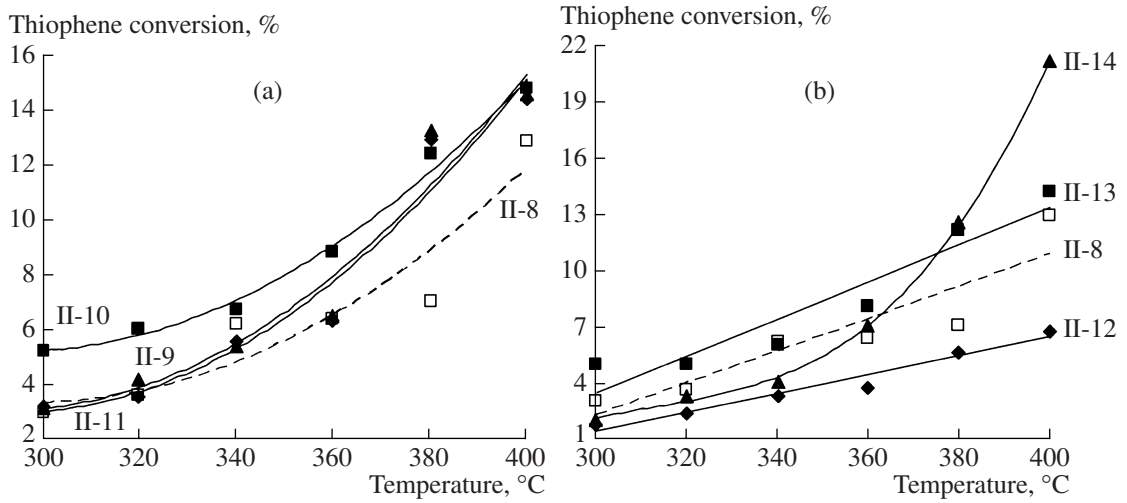

Fig. 3. Thiophene conversion versus temperature for Anderson HPC–based Ni-*X*Mo_6(S)/γ-Al_2O_3 catalyst samples (a) II-9 to II-11 and (b) II-12 to II-14 and over an APM-based Ni-Mo_7(S)/γ-Al_2O_3 catalyst (II-8).

highest HA (62.9 rel. %) for sample II-11. Residual sulfur in the diesel fuel being dibenzothiophenes, benzonaphthothiophenes, and their derivatives, their elimination requires prehydrogenation; therefore, the high hydrogenation activity of this catalyst provided for its high HDSA.

Samples II-8 and II-9 demonstrated practically identical hydrogenation activities. However, different residual percentages of bicyclic aromatic hydrocarbons (BAH) and tricyclic aromatic hydrocarbons (TAH) in the hydrogenizates were obtained over these catalysts (Table 2). In the hydrogenizates obtained in testing catalyst II-8, BAH percentages were lower than in the hydrogenizates of catalyst II-9. On the contrary, TAH percentages in the hydrogenizates of catalyst II-9 were lower than in hydrogenizates of catalyst II-8. Thus, the high degree of TAH hydrogenization over catalyst II-9 increased BAH percentages in hydrogenizates; it is for this reason that the degree of BAH hydrogenization over catalyst II-9 was lower than over the reference (sample II-8). The degree of PAH hydrogenization over catalyst II-10 was higher than over samples II-8 and II-9 but lower than on catalyst II-11. Thus, the nature of the HPC determines the activity of Ni-*X*Mo_6(S)/γ-Al_2O_3 catalysts with *X* = Al, Ga, and In, which increases in the order Al < Ga < In.

Ni-*X*Mo_6(S)/γ-Al_2O_3 catalysts with *X* = Co, Fe, and Ni (samples II-12 to II-14) had higher HDSA than the reference (sample II-8) over the entire range of the temperatures studied (Fig. 5a). Catalysts II-12 and II-13 (prepared from $FeMo_6$-HPC and $CoMo_6$-HPC, respectively) had similar HDSAs. Catalyst II-14 prepared from $NiMo_6$-HPC was more active. The HDSA increased in the order Fe < Co < Ni.

Of the set II catalysts, catalyst II-14 synthesized using $NiMo_6$-HPC had the highest HA (Fig. 5b). The HAs of catalysts II-12 and II-8 were at one level; the activity of $CoMo_6$-HPC-based catalyst II-13 was the lowest.

The performance stability of a catalyst can be indirectly ascertained as the coke percentage formed on its surface during the reaction (Table 1). The lowest coke percentage (1.5 wt %) was contained in the Ni-Mo_6-HPC-based catalyst (sample II-14); a little more coke (2.1–2.5 wt %) was contained in the reference (sample II-8) and catalysts II-9 and II-13. $InMo_6$-HPC and $GaMo_6$-HPC catalysts contained 6.4 and 6.8 wt % coke, respectively. The highest coke percentage (11.4 wt %) was formed over the catalyst prepared from $FeMo_6$-HPC.

Thus, heteroatom *X* in such supported complex catalytic systems can play its role both during the manufacture of the catalyst first in the oxide and then in the sulfide form and in the catalytic action of the mixed sulfide phase. In this context, it is relevant to mention a recent work by Lamonier et al. [23]. They used high-resolution electron microscopy to demonstrate the high dispersion of the active sulfide phase immobilized on γ-Al_2O_3 prepared from cobalt 10-HPC ($[Co_2Mo_{10}O_{38}H_4^{6-}]$) compared to the sulfide phase of a conventionally manufactured catalyst. In the latter, large crystallites of poorly sulfidized MoO_3 were observed, whereas the HPC-based catalyst contained rather small crystallites. X-ray photoelectron spectroscopy showed no differences in the position or shape of the Co_{2p} peak. The $E(Co_{2p})$–$E(Mo_{3d})$ binding energy for both catalysts is 550.2 eV, which is characteristic of terminal Co positions in the "CoMoS" model [34]. Our explanation of these results is as follows. Sulfidizing considerably changes the crystal structure of oxide precursors; the cubic lattice of the heteroatom-doped MoO_3 phase [35] or the heteropoly anion structure undestroyed by calcining transforms into the MoS_2 tri-

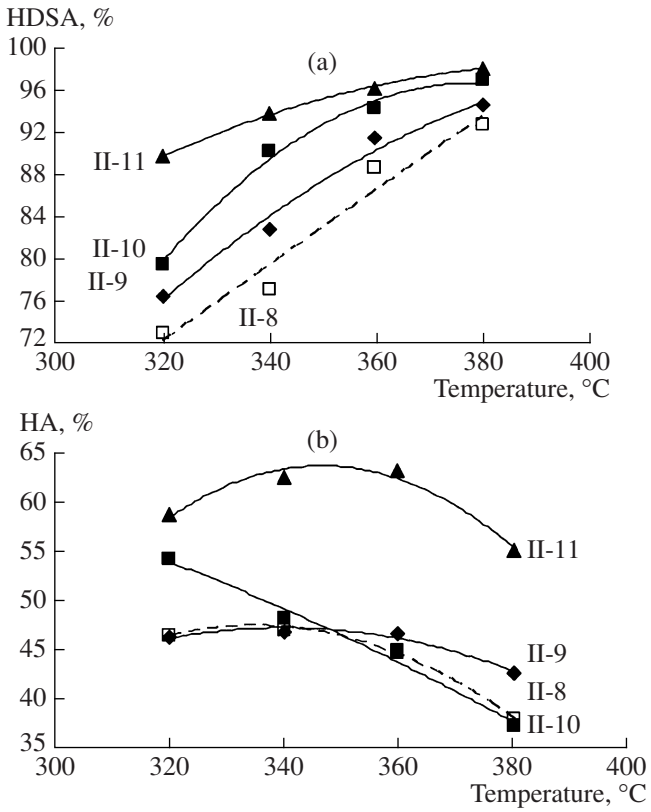

Fig. 4. (a) Hydrodesulfurization and (b) hydrogenation activities of Anderson HPC–based Ni-XMo$_6$(S)/γ-Al$_2$O$_3$ catalysts (samples II-9 to II-11) and an APM-based Ni-Mo$_7$(S)/γ-Al$_2$O$_3$ catalyst (sample II-8) versus the temperature of diesel fuel hydrorefining.

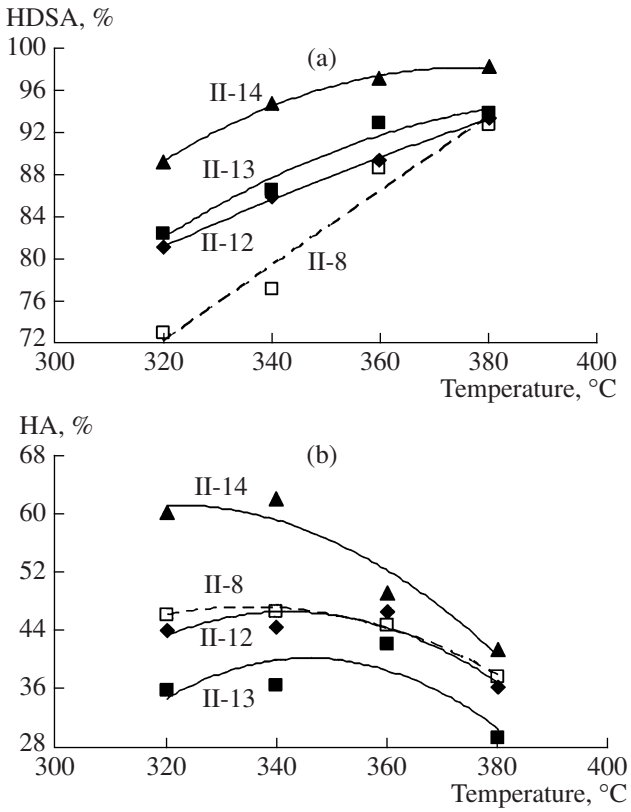

Fig. 5. (a) Hydrodesulfurization and (b) hydrogenation activities of Anderson HPC–based Ni-XMo$_6$(S)/γ-Al$_2$O$_3$ catalysts (samples II-12 to II-14) and an APM-based Ni-Mo$_7$(S)/γ-Al$_2$O$_3$ catalyst (sample II-8) versus the temperature of diesel fuel hydrorefining.

gonal lattice. Heteroelement atoms migrate to terminal positions with the attendant destruction of the initial crystallites and increase in the relative dispersion of the sulfide phase. In cases of HPCs where heteroelements in the coordination sphere are not conventional promoters for sulfide catalysts (that is, nickel or cobalt), the role of the heteroelements also consists of changing the chemical composition of the sulfide active phase, and, through this, its catalytic properties. As known from [36–38], a promoter in a mixed sulfide phase like Ni(Co)Mo(W)S functions as an electron-density donor for atoms of the major active component (molybdenum or tungsten). An increase in electron density on molybdenum antibonding orbitals weakens Mo–S bonds in the active phase, which is manifested as a decrease in the energy required for generating coordinatively unsaturated active sites. The donor ability increases with increasing number of electrons at the outer electronic shells in increasing order of atomic numbers from left to right for fourth-period transition metals (Fe, Co, and Ni) and from top down for boron-family elements (Al, Ga, and In); the increased donor ability evidently influences the catalytic activity of our synthesized catalysts. Thus, the enhanced activity of catalysts manufactured from HPCs can be explained by the increased relative dispersion of the active sulfide phase and the synergistic effect of heteroelements and active components.

CONCLUSIONS

(1) XMo$_6$(S)/γ-Al$_2$O$_3$ and Ni-XMo$_6$(S)/γ-Al$_2$O$_3$ catalysts were prepared on the basis of Anderson heteropoly compounds, where X = Al, Ga, In, Fe, Co, or Ni. Their activity in thiophene hydrogenolysis and diesel fuel hydrorefining was tested on a flow-through setup.

(2) XMo$_6$(S)/γ-Al$_2$O$_3$ catalysts with X = Al, Ga, and In demonstrate practically identical thiophene hydrogenolysis activities. The activities of XMo$_6$(S)/γ-Al$_2$O$_3$ catalysts with X = Fe, Co, and Ni are arranged in the following order depending on the central heteroatom: Fe < Co < Ni.

(3) Nickel promotion increases the activity of the catalyst. Thiophene conversions over Ni-XMo$_6$(S)/γ-Al$_2$O$_3$ catalysts with X = Al, Ga, and In are approximately equal; those for the catalysts with X = Fe, Co, and Ni are arranged in the same order as for the unpromoted catalysts. The Ni-XMo$_6$(S)/γ-Al$_2$O$_3$ catalysts with X = Al, Ga, and In are arranged in the following order of

increasing diesel fuel hydrodesulfurization activity as a function of the heteroatom: Al < Ga < In; for the catalysts with a iron triad element, the increasing order of activity is Fe < Co < Ni.

(4) In summary, we have shown that the nature of the precursor HPC determines the hydrogenation and hydrodesulfurization activities of the catalyst.

(5) The highest hydrogenation and hydrodesulfurization activities were observed for catalysts prepared on the basis of $InMo_6$-HPC and $NiMo_6$-HPC. The residual sulfur percentage in hydrogenizates obtained at 320°C on these catalysts is 2.5 times lower than conventional APM-based catalysts. The degree of PAH hydrogenation is 15–16 rel. % higher.

ACKNOWLEDGMENTS

P.A. Nikul'shin acknowledges financial support for dissertation from Haldor Topsøe A/S.

REFERENCES

1. Kozhevnikov, I.V., *Usp. Khim.*, 1993, vol. 62, no. 5, p. 510.
2. Navalikhina, M.D., Malkina, I.L., and Garanin, V.I., *Neftekhimiya*, 1990, vol. 30, p. 26.
3. Navalikhina, M.D., Kagan, D.N., and Shpil'rain, E.E., *Preprint of Joint Institute for High Temperatures*, Moscow, 2003, no. 8-472.
4. Navalikhina, M.D. and Krylov, O.V., *Kinet. Katal.*, 2001, vol. 42, no. 2, p. 294 [*Kinet. Catal.* (Engl. Transl.), vol. 42, no. 2, p. 264].
5. Navalikhina, M.D., Proskurnin, A.M., and Krylov, O.V., *Katal. Prom–sti.*, 2001, no. 1, p. 39.
6. Spojakina, A.A., Kostova, N.G., Yuchnovski, I.N., Shopov, D.M., Yurieva, T.M., and Shokhireva, T.Kh., *Appl. Catal.*, 1988, vol. 39, p. 333.
7. Spojakina, A., Damyanova, S., Shopov, D., Shokireva, T.Kh., and Yurieva, T.M., *React. Kinet. Catal. Lett.*, 1985, vol. 27, p. 333.
8. Spojakina, A.A., Gigov, B., and Shopov, D.M., *React. Kinet. Catal. Lett.*, 1982, vol. 19, no. 2, p. 11.
9. Spozhakina, A.A., Kostova, N.G., Tsolovski, I.A., and Shopov, D.M., *Kinet. Katal.*, 1982, vol. 23, no. 2, p. 456.
10. Shokhireva, T.Kh., Yurieva, T.M., Altynnikov, A.A., Anufrienko, V.F., Plyasova, L.M., Litvak, G.S., Spojakina, A.A., and Kostova, N., *React. Kinet. Catal. Lett.*, 1992, vol. 47, p. 177.
11. Okamoto, Y., Gomi, I., Mori, Y., Inamaka, T., and Teranishi, S., *React. Kinet. Catal. Lett.*, 1983, vol. 22, p. 417.
12. Tomina, N.N., *Cand. Sci. (Eng.) Dissertation*, Ufa: Ufa Petroleum Inst., 1990.
13. Tomina, N.N., Pimerzin, A.A., Loginova, A.N., Sharikhina, M.A., Zhilkina, E.O., and Eremina, Yu.V., *Neftekhimiya*, 2004, vol. 44, no. 4, p. 274 [*Pet. Chem.* (Engl. Transl.), vol. 44, no. 4, p. 246].
14. Tomina, N.N., Pimerzin, A.A., Eremina, Yu.V., Tsvetkov, V.S., and Pil'shchikov, V.A., *Izv. Vyssh. Uchebn. Zaved., Khim. Khim. Tekhnol.,* 2005, vol. 48, no. 10, p. 12.
15. Griboval, A., Blanchard, P., Gengembre, L., Fournier, M., Dubois, J.L., and Bernard, J.R., *J. Catal.*, 1999, vol. 188, p. 102.
16. Maitra, A.M., Cant, N.W., and Trimm, D.L., *Appl. Catal.*, 1989, vol. 48, no. 1, p. 187.
17. Cabello, C.I., Munoz, M., Payen, E., and Thomas, H.J., *Catal. Lett.*, 2004, vol. 92, p. 69.
18. Cabello, C.I., Cabrerizo, F.M., Alvarez, A., and Thomas, H.J., *J. Mol. Catal. A: Chem.*, 2002, vol. 186, p. 89.
19. Cabello, C.I., Botto, I.L., and Thomas, J.H., *Appl. Catal., A*, 2000, vol. 197, p. 79.
20. Pettiti, I., Botto, I.L., Cabello, C.I., Colonna, S., Faticanti, M., Minelli, G., Porta, P., and Thomas, J.H., *Appl. Catal., A*, 2001, vol. 220, p. 113.
21. Nikul'shin, P.A., Eremina, Yu.V., Tomina, N.N., and Pimerzin, A.A., *Neftekhimiya*, 2006, vol. 46, no. 5, p. 371 [*Pet. Chem.* (Engl. Transl.), vol. 46, no. 5, p. 343].
22. Nikul'shin, P.A., Tomina, N.N., and Pimerzin, A.A., *Izv. Vyssh. Uchebn. Zaved., Khim. Khim. Tekhnol.*, 2007, vol. 50, no. 9, p. 54.
23. Lamonier, C., Martin, C., Mazurelle, J., Harle, V., Guillaume, D., and Payen, E., *Appl. Catal., B*, 2007, vol. 70, p. 548.
24. Nikitina, E.N., *Geteropolisoedineniya* (Heteropoly Compounds), Moscow: Goskhimizdat, 1962.
25. *Handbuch der preparativen anorganischen Chemie*, von Brauer, G., Ed., Stuttgart: Ferdinand Enke, 1981.
26. Eremina, Yu.V., *Cand. Sci. (Chem.) Dissertation*, Samara: Samara State Technical Univ., 2006.
27. Siryuk, A.G. and Zimina, K.I., *Khim. Tekhnol. Topl. Masel*, 1963, no. 2, p. 52.
28. Rybak, B.M., *Analiz nefti i nefteproduktov* (Analysis of Petroleum and Petroleum Products), Moscow: Gostoptekhizdat, 1962.
29. Davydov, A.A. and Goncharova, O.I., *Usp. Khim.*, 1993, vol. 62, no. 2, p. 118.
30. Kazanskii, L.P. and Golubev, A.M., in *Khimiya soedinenii Mo(VI) and W(VI)* (Chemistry of Mo(VI) and W(VI) Compounds), Novosibirsk: Nauka, 1979, p. 66.
31. Yurchenko, E.N., *Metody molekulyarnoi spektroskopii v khimii koordinatsionnykh soedinenii i katalizatorov* (Methods of Molecular Spectroscopy in the Chemistry of Coordination Compounds and Catalysts), Novosibirsk: Nauka, 1986.
32. La Ginestra, A., Giannetta, A., and Fiorucci, F., *Gazz. Chim. Ital.*, 1968, vol. 98, p. 1197.
33. Cattier, X., Lambert, J.-F., Kuba, S., Knozinger, H., and Che, M., *J. Mol. Struct.*, 2003, vol. 656, p. 231.
34. Topsoe, H., *Appl. Catal., A*, 2007, vol. 322, p. 3.
35. Varfolomeev, M.B., Burljaev, V.V., Toporenskaja, T.A., Lunk, H.-J., Wilde, W., and Hilmer, W., *Z. Anorg. Allg. Chem.*, 1981, no. 472, p. 185.
36. Harris, S. and Chianelli, R.R., *J. Catal.*, 1986, vol. 98, p. 17.
37. Chianelli, R.R., Berhault, G., Raybaud, P., Kasztelan, S., Hafner, J., and Toulhoat, H., *Appl. Catal., A*, 2002, vol. 227, p. 83.
38. Chianelli, R.R., *Oil Gas Sci. Technol.*, 2006, vol. 61, p. 503.